数理解析研究所講究録
第 710 巻 1989 年 127-144

Bifurcation Analysis of Shilnikov's Chaos

R.Fujimoto†, A.Hotta†, R.Tokunaga†, M.Komuro†† and T.Matsumoto†
(藤本竜一)(堀田篤宏)(徳永隆治)(小室元政) (松本隆)

Abstract

Detailed bifurcation analysis is given near homoclinic orbit of a picewise-linear flow on $\mathbb{R}^3$. The significance of the Shilnikov conditions are studied.

1.INTRODUCTION

Consider the 2-region picewise-linear system in $\mathbb{R}^3$

$$\frac{dX}{dt} = AX + \frac{1}{2}p\{|<\alpha,X> - 1| + (<\alpha, X> - 1)\} \qquad (1.1)$$

where

$$A = \begin{bmatrix} \sigma_0 & -\omega_0 & 0 \\ \omega_0 & \sigma_0 & 0 \\ 0 & 0 & \gamma_0 \end{bmatrix}, p = \begin{bmatrix} p_1 \\ p_2 \\ p_3 \end{bmatrix}, \alpha = \begin{bmatrix} 1 \\ 0 \\ 1 \end{bmatrix}$$

which is the normal form developed in [1],[2].

If the following conditions are satisfied (the Shilnikov conditions [3],[4]) :

(a) $|\sigma_0| < \gamma_0$

(b) there exists a *homoclinic orbit* through the origin,

† Department of Electrical Engineering, Waseda University, Tokyo 160, Japan

†† Department of Mathematics, Numazu College of Technology, Numazu 410, Japan

then every neighborhood of the homoclinic orbit contains infinitely many periodic orbits of saddle type. (An orbit which tends to the origin as $t \to \pm\infty$ is called homoclinic.)

In fact, the homoclinic orbit is a limit of a family of saddle type periodic orbits. Fig.1 shows the case in point on the σ_1-period space. Fig.2 shows these periodic orbits corresponding to (a)-(d) in Fig.1.

The purpose of this paper is to study the significance of the Shilnikov conditions in the bifurcation structures near homoclinicity. In particular, we will study what happens when (a) and/or (b) is violated.

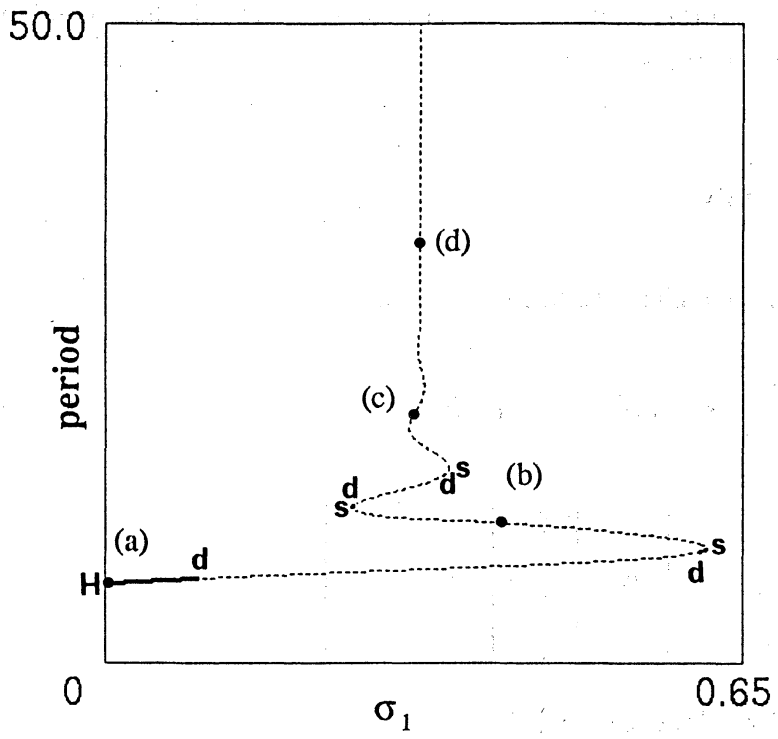

Fig.1 Periodic orbits approach to the homoclinic orbit. ($\sigma_0 = -0.3$)

——— stable or unstable periodic orbit

- - - - - - saddle type periodic orbit

s : saddle node bifurcation

d : period doubling bifurcation

H : Hopf bifurcation

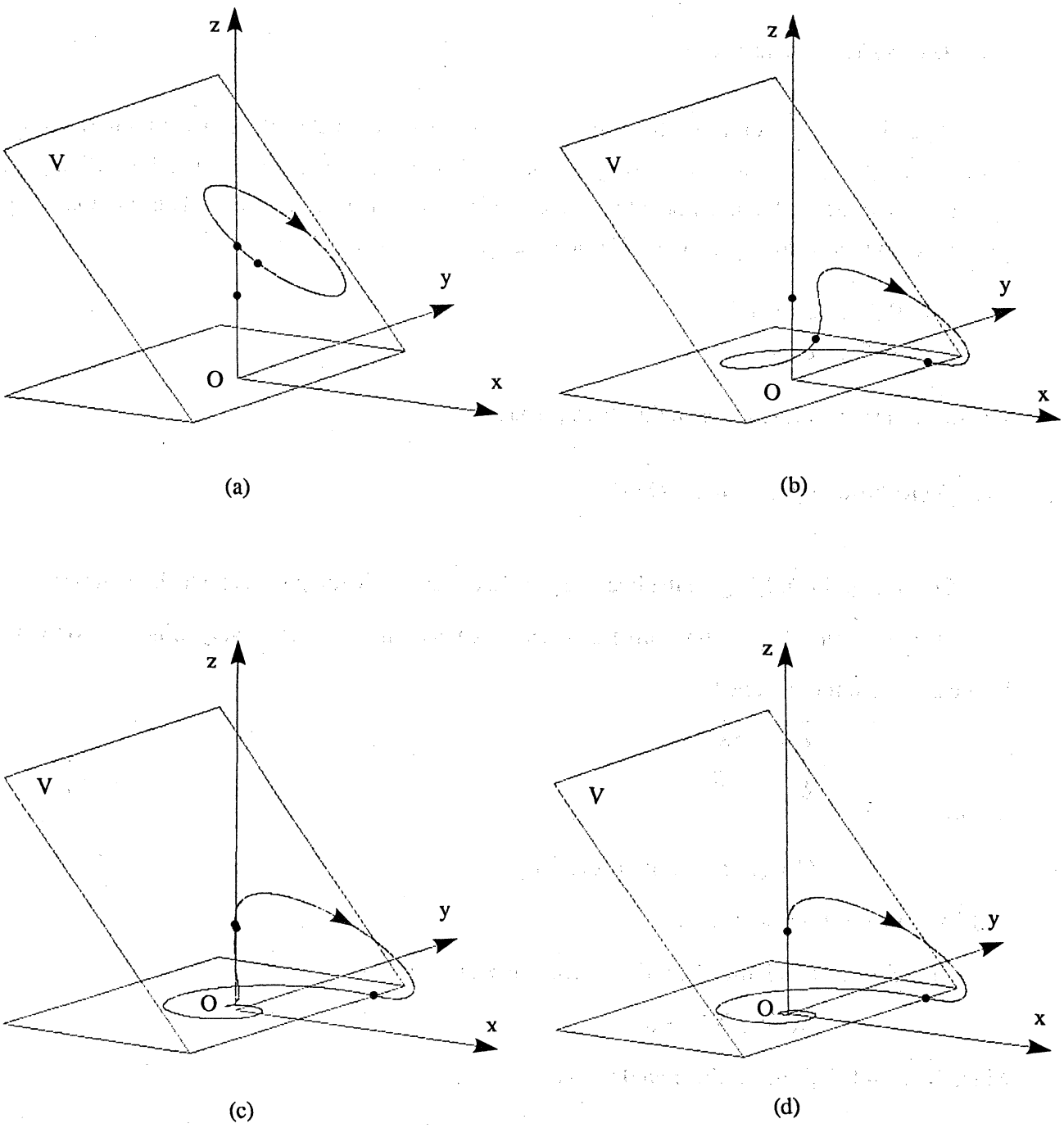

Fig.2 Periodic orbit changes the shape like a homoclinic orbit.

2.GEOMETRIC STRUCTURE AND BIFURCATION EQUATIONS

2.1 Geometric Structure

Fig.3 shows the geometric structure of (1.1). At those parameter values we are interested the system has two equilibrium points, origin O and P. Eigenvalues at O are denoted by $\sigma_0 \pm j\omega_0$ and γ_0, and eigenvalues at P are denoted by $\sigma_1 \pm j\omega_1$ and γ_1. Note that vector **p** in (1.1) is automatically determined by these six eigenvalues. Throughout this paper, we will fix

$$\gamma_0 = 0.5 \ , \ \omega_0 = 1.0$$
$$\gamma_1 = -0.5 \ , \ \omega_1 = 1.0$$

and study various bifurcations in the (σ_1,σ_0)-space.

2.2 Equations Of Periodic Orbits

Consider point $\tilde{\mathbf{X}}$ lying on the boundary V. Let $\tilde{\mathbf{Y}}$ and $\tilde{\mathbf{Z}}$ lie the points at which the trajectory starting from $\tilde{\mathbf{X}}$ hits V again at positive time s and negative time -t, respectively. Since the system is linear in each region, one has

$$\tilde{\mathbf{Y}} = e^{\mathbf{C}s}\tilde{\mathbf{X}}$$
$$\tilde{\mathbf{Z}} = e^{-\mathbf{A}t}\tilde{\mathbf{X}} \qquad (2.1)$$

where

$$\mathbf{C} = \mathbf{A}^{-1}\mathbf{B}\mathbf{A} \ , \ \mathbf{B} = \mathbf{A}+\mathbf{p}^{T}\alpha$$

and ${}^{T}\alpha$ indicates transpose of α.

If the orbit is periodic, then $\tilde{\mathbf{Y}} = \tilde{\mathbf{Z}}$ which is equivalent to

$$(e^{-\mathbf{A}t}-e^{\mathbf{C}s})\tilde{\mathbf{X}} = 0$$

Since $\tilde{\mathbf{X}}, \tilde{\mathbf{Y}}$ and $\tilde{\mathbf{Z}}$ all lie on the boundary V,

$$<\alpha,\tilde{\mathbf{X}}> = 1, \ <\alpha,e^{\mathbf{C}s}\tilde{\mathbf{X}}> = 1, \ <\alpha,e^{-\mathbf{A}t}\tilde{\mathbf{X}}> = 1$$

Therefore

$$\tilde{\mathbf{X}} = (\mathbf{e}_1{}^{T}\alpha e^{-\mathbf{A}t} + \mathbf{e}_2{}^{T}\alpha e^{\mathbf{C}s} + \mathbf{e}_3{}^{T}\alpha)^{-1} \ {}^{T}(1,1,1) = \mathbf{k}(s,t)\,\mathbf{h} \qquad (2.2)$$

where

$$\mathbf{e}_1 = {}^{T}(1,0,0) \ , \ \mathbf{e}_2 = {}^{T}(0,1,0) \ , \ \mathbf{e}_3 = {}^{T}(0,0,1) \ , \ \mathbf{h} = {}^{T}(1,1,1)$$

Consequently, a *periodic orbit* is characterized by

$$(e^{-At}-e^{Cs})\mathbf{k}(s,t)\mathbf{h} = 0 \qquad (2.3)$$

Remark. There are only two (out of three) independent equations in (2.3) because $\tilde{\mathbf{X}}, \tilde{\mathbf{Y}}$ and $\tilde{\mathbf{Z}}$ all lie on V, a two dimensional subspace.

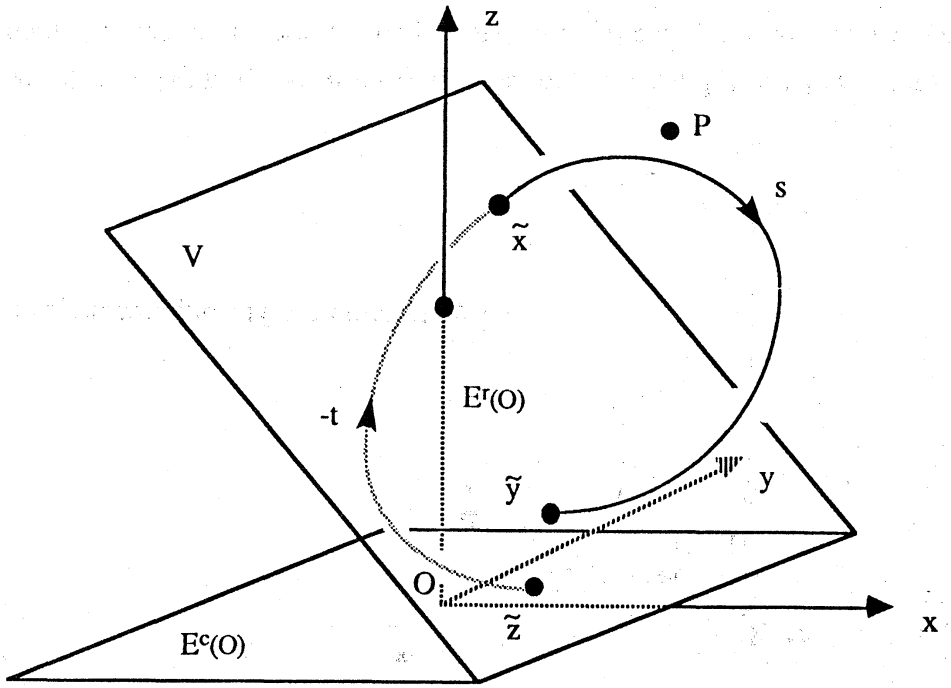

Fig.3 The Poincaré return map

Notations associated with Fig.3

O : equilibrium point

P : equilibrium point

$E^c(O)$: 2-dimensional eigenspace corresponding to complex eigenvalue $\sigma_0 \pm \omega_0$ at O

$E^r(O)$: 1-dimensional eigenspace corresponding to real eigenvalue γ_0 at O

V : boundary

2.3 Homoclinic Bifurcation Equations

If a trajectory starting from the point (0,0,1) hits $E^c(O)$ on the boundary V, then it is a homoclinic orbit through the origin.(Fig.4) The *homoclinicity* is characterized by

$$
\begin{aligned}
&{}^T\alpha e^{Cs_0} e_3 = 1 \\
&{}^T\alpha e_3 e^{Cs_0} e_3 = 0
\end{aligned}
\qquad (2.4)
$$

where s_0 is the time at which the trajectory hits $V \cap E^c(O)$ starting from ${}^T(0,0,1)$. Of course more complicated homoclinicites can also be characterized by equations similar to (2.4).

Fig.5 shows set of point in the (σ_1,σ_0)-space where homoclinicity occurs which is called the *homoclinic bifurcation set.* Fig.6 shows the trajectories corresponding to points (a)-(e) in Fig.5.

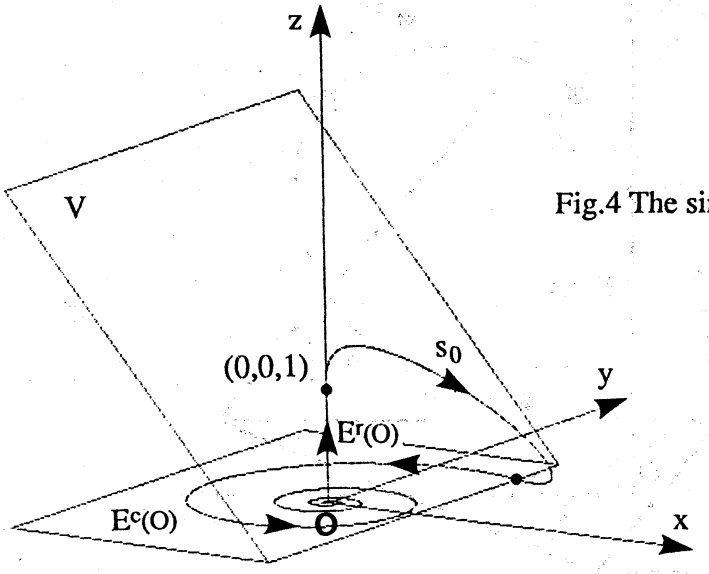

Fig.4 The simplest type of homoclinic orbit

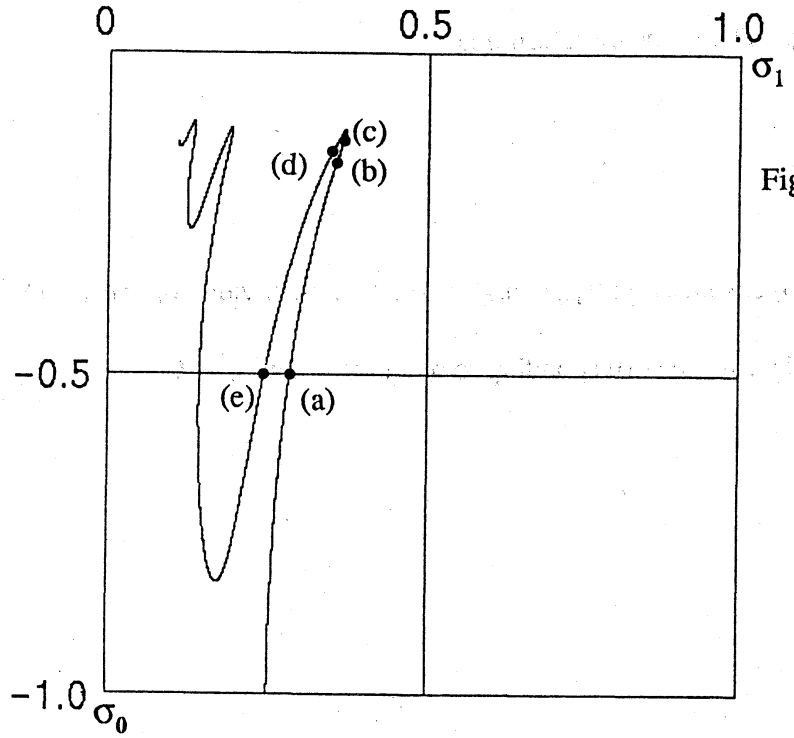

Fig.5 Homoclinic bifurcation set

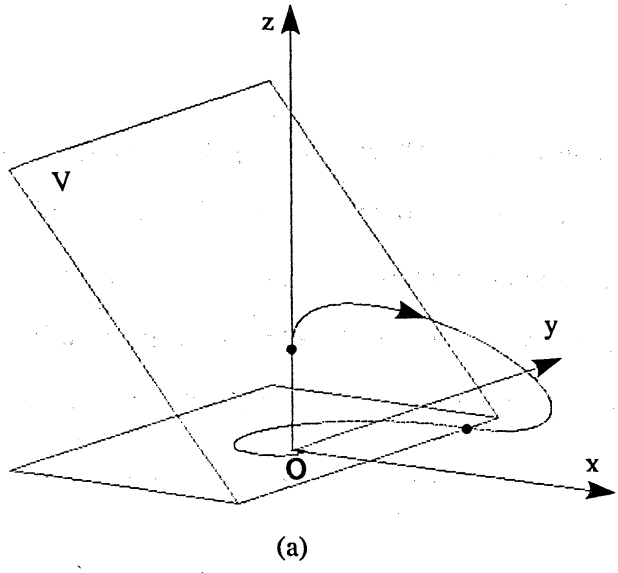

(a)

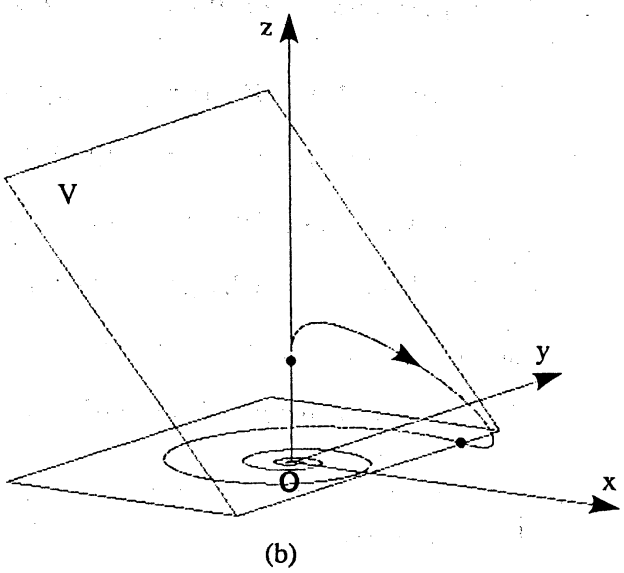

(b)

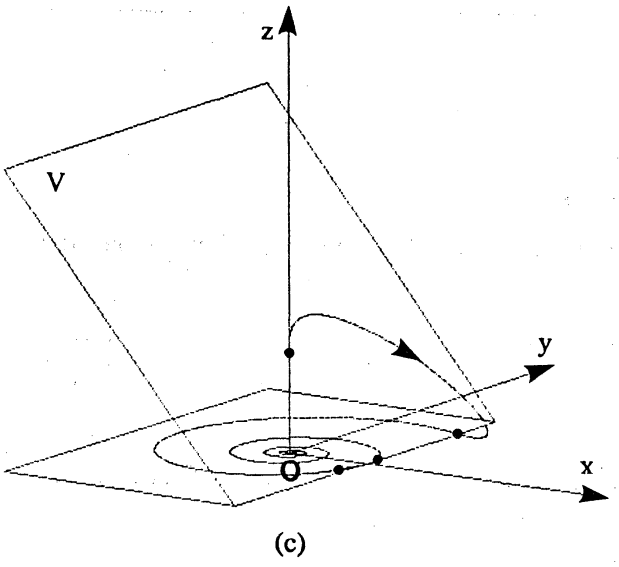

(c)

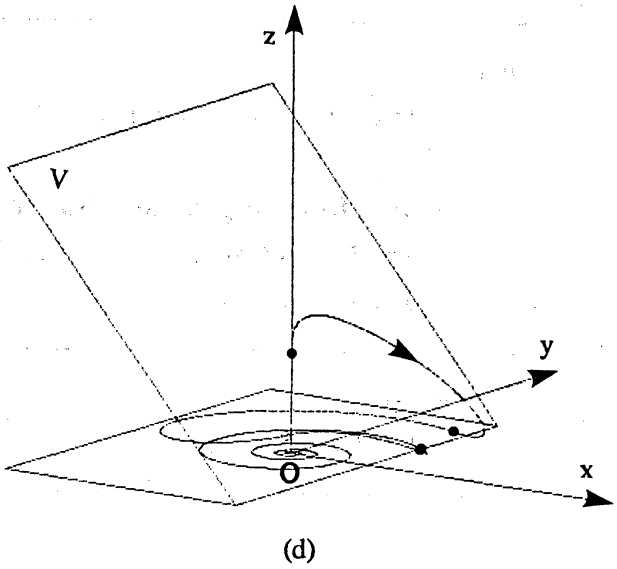

(d)

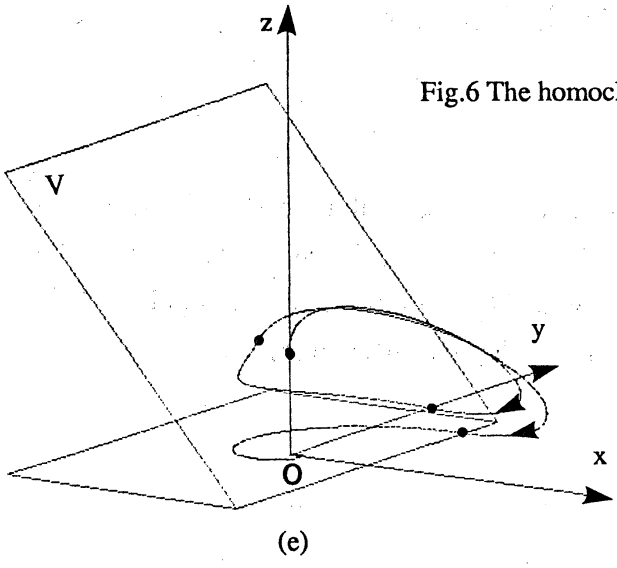

(e)

Fig.6 The homoclinic orbit from Fig.5 illustrated at the points (a)-(e)

2.4 Bifurcation Equations Of Periodic Orbit

A. Saddle Node Bifurcation Equation

It is shown rigorously in [1],[2] that eigenvalues of the Poincaré return map on V is given by the eigenvalues of $e^{At}e^{Bs}$. It should be noted that this is not as trivial as it looks because *t and s vary as* $\tilde{X}$ *varies* . One has to use the implicit function theorem. Note that if $\tilde{X}$ is a periodic orbit, one of the three eigenvalues of $e^{At}e^{Bs}$ is **always** 1. Since a **saddle node bifurcation** is characterized by the fact that one of the remaining two eigenvalues is 1, it is characterized by

$$\begin{aligned} &2\text{-}T+D = 0 \\ &(e^{-At}\text{-}e^{Cs})\mathbf{k}(s,t)\mathbf{h} = 0 \end{aligned} \qquad (2.5)$$

where

$T = \text{trace}(e^{At}e^{Bs})$, $D = \det(e^{At}e^{Bs})$.

B. Period Doubling Bifurcation Equation

A **period doubling bifurcation** is characterized by the fact that one of the remaining eigenvalues being -1:

$$\begin{aligned} &T+D=0 \\ &(e^{-At}\text{-}e^{Cs})\mathbf{k}(s,t)\mathbf{h} = 0. \end{aligned} \qquad (2.6)$$

3. BIFURCATIONS NEAR HOMOCLINICITY

3.1 Global Bifurcations

Fig.7(a) (resp.(b)) gives **saddle-node** (resp. **period-doubling**) bifurcation set corresponding to the **right most portion** of the homoclinic bifurcation set given by Fig.5, on which (a),(b) and(c) lie. Fig.7(c)(resp. (d)) shows saddle-node(resp. period-doubling) bifurcation set corresponding to the next portion of Fig.5 on which points (d) and (e) lie.

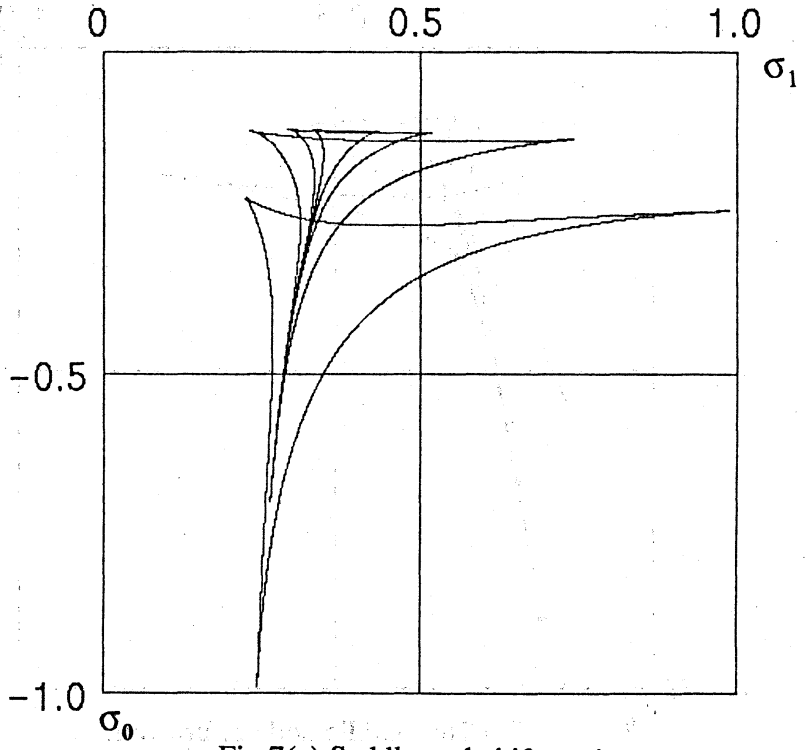

Fig.7(a) Saddle node bifurcation

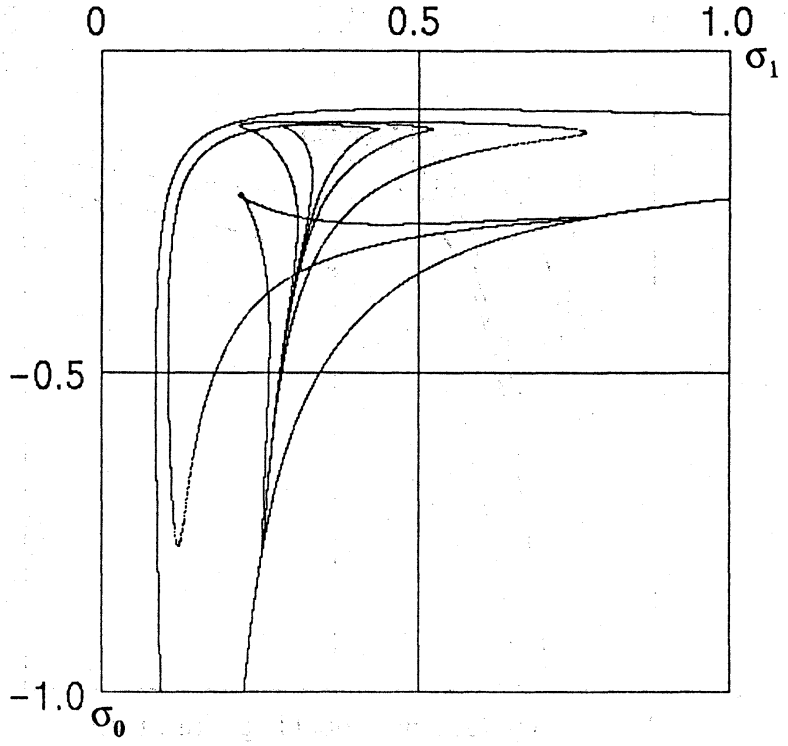

Fig.7(b) Period doubling bifurcation

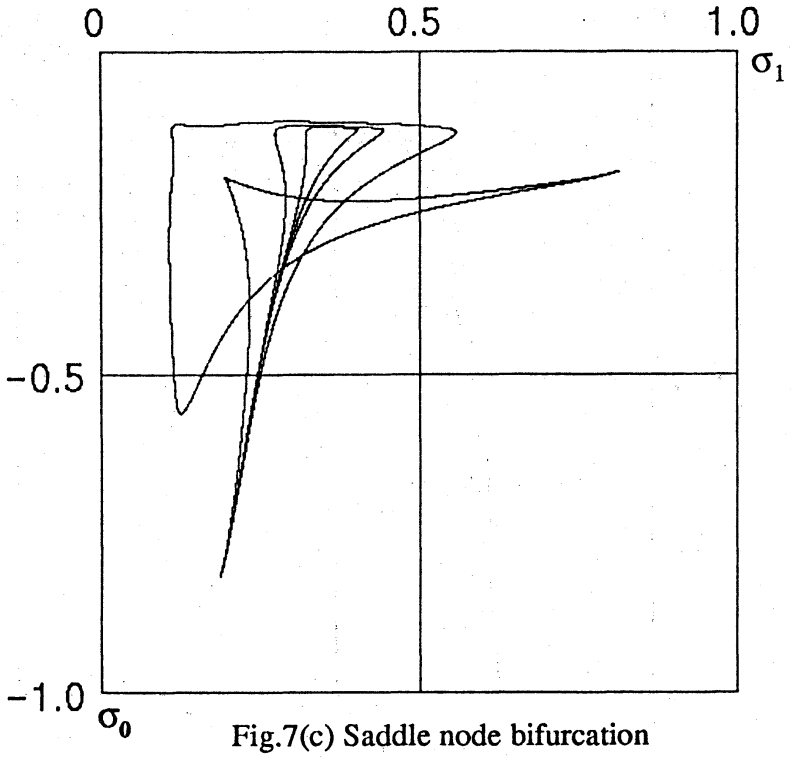

Fig.7(c) Saddle node bifurcation

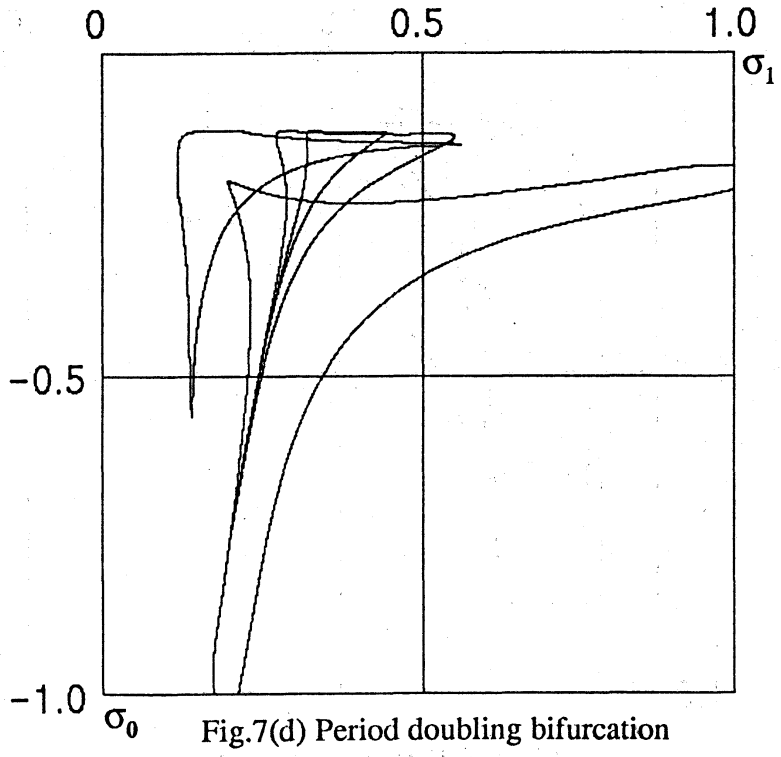

Fig.7(d) Period doubling bifurcation

3.2 Local Bifurcations

A.When the Shilnikov conditions are satisfied.

When the Shilnikov conditions are satisfied, that is

(a) $|\sigma_0| < \gamma_0$

(b) there exists a homoclinic orbit through the origin,

then there are infinitely many saddle node bifurcation sets and period doubling bifurcation sets near homoclinicity. Fig.8 shows a blown up picture of Fig.5 on which Fig.7(a),(b) are superimposed. This tells us the following:

> If the Shilnikov conditions are satisfied, then saddle node bifurcation sets and period doubling bifurcation sets **accumulate to homoclinic bifurcation set** in pairs.

Next, we show a detail of Fig.8 in Fig.9 which illustrates Hopf bifurcation set of periodic orbit. This Hopf bifurcation set is the boundary between attractive periodic orbit and repelling periodic orbit.

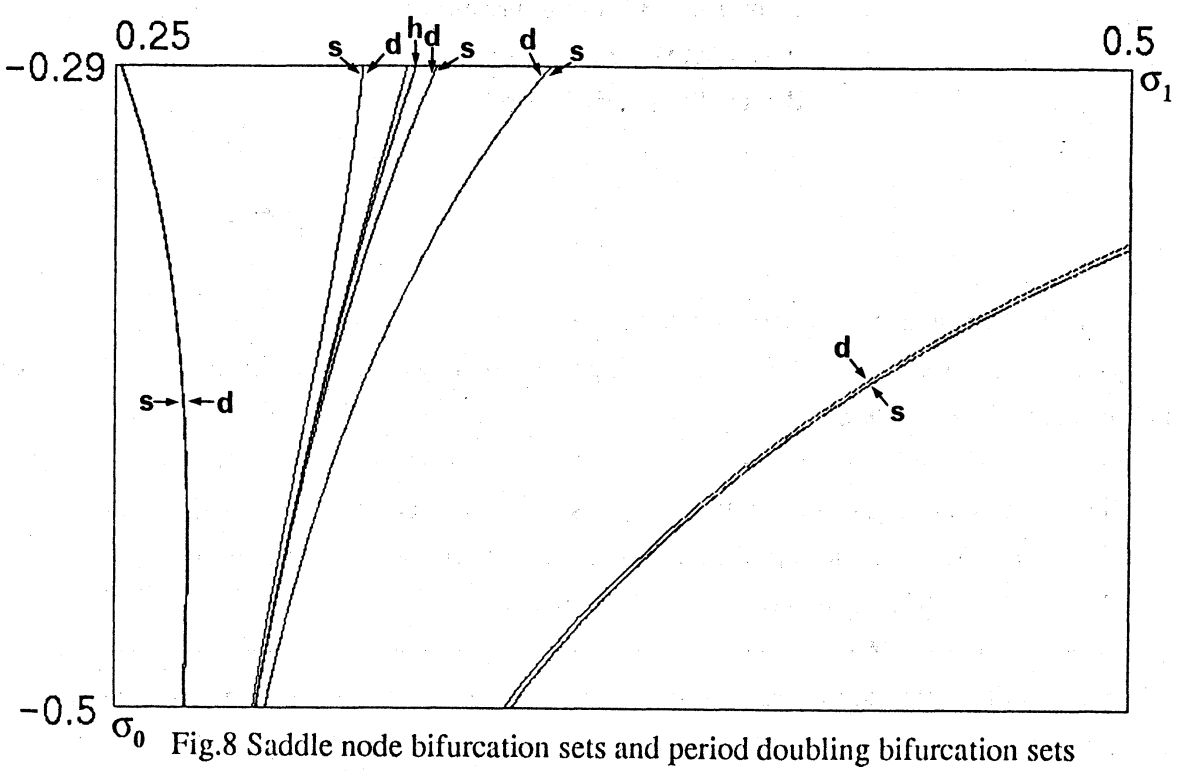

Fig.8 Saddle node bifurcation sets and period doubling bifurcation sets

s : saddle node bifurcation set

d : period doubling bifurcation set

h : homoclinic bifurcation set

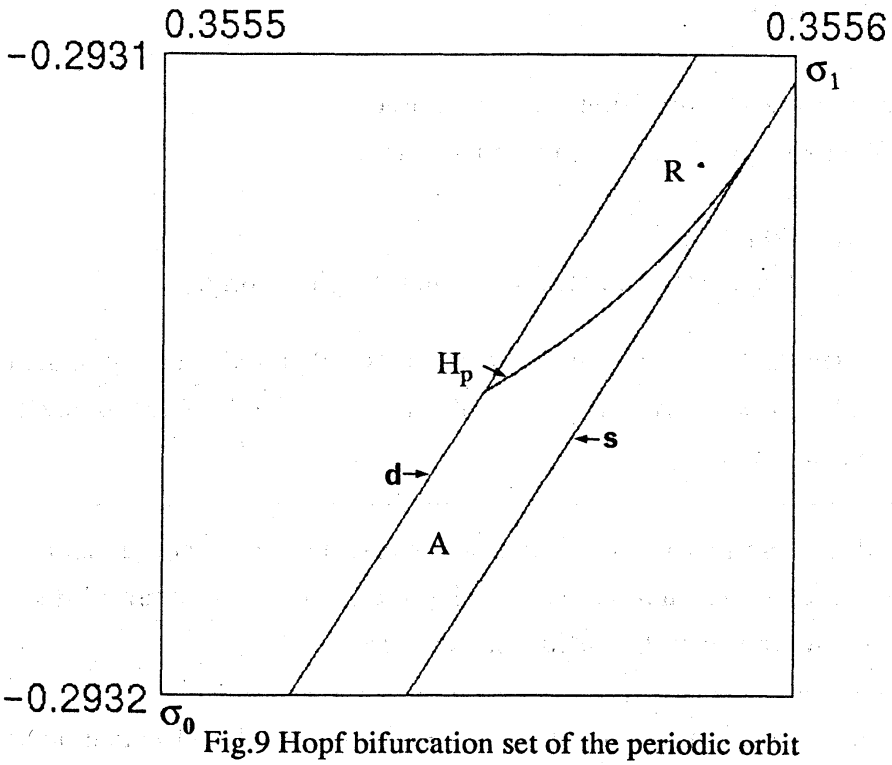

Fig.9 Hopf bifurcation set of the periodic orbit

H_p : Hopf bifurcation set of the periodic orbit

s : saddle node bifurcation set

d : period doubling bifurcation set

A : attractive periodic orbit

R : repelling periodic orbit

B.When the Shilnikov condition (a) is violated.

Fig.10 shows the (σ_1,σ_0)-bifurcation diagram when $|\sigma_0| \geq \gamma_0$ while there still exists a homoclinic orbit. One sees that

> If the Shilnikov condition (a) does not hold then the saddle node and period doubling bifurcation sets *vanish in pairs*. Further more saddle node bifurcation set ends with a ***cusp*** point.

In the present situation, therefore, there are only a finite number of periodic orbits near homoclinicity.

Remark. Observe that the cusp point of saddle node bifurcation sets accumulate to a point where homoclinic bifurcation set intersects the line $\sigma_0 = -\gamma_0$.

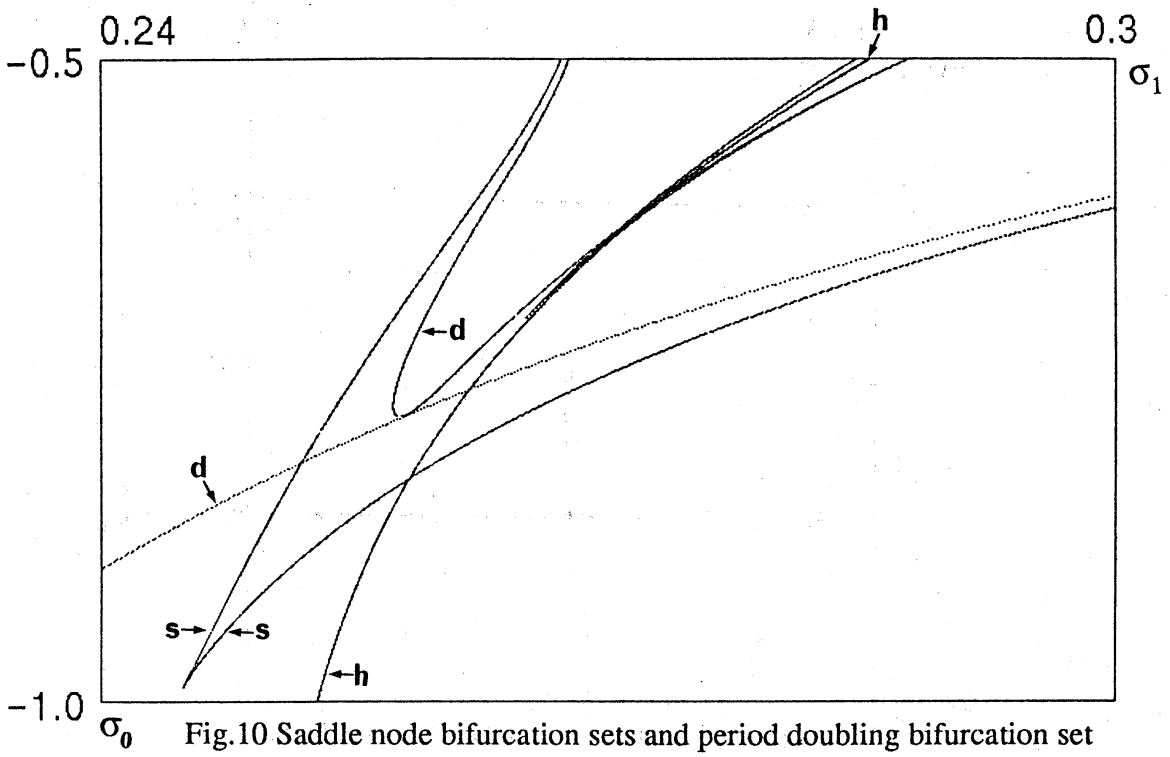

Fig.10 Saddle node bifurcation sets and period doubling bifurcation set

s : saddle node bifurcation set

d : period doubling bifurcation set

h : homoclinic bifurcation set

C.When the Shilnikov condition (b) is violated.

Consider the case when there is no homoclinic orbit while $|\sigma_0| < \gamma_0$ still holds. First let us look at the blown up homoclinic bifurcation set given by Fig.11. Note that at $\sigma_0 = \sigma_0^1$, there are two homoclinic orbits while at $\sigma_0 = \sigma_0^2$, there is no homoclinicity. Fig.12(a)(resp. (b)) shows the saddle node(resp. period doubling) bifurcation set corresponding to the "right-hand portion" of the curve given in Fig.11, while Fig.12(c) and (d) give the bifurcations corresponding to the "left-hand portion". All the pictures are superimposed in Fig.12(e). Our observation is the following:

> If the Shilnikov condition (b) is violated, then saddle node bifurcation sets and period doubling bifurcation sets **vanish one by one.** Furthermore,the "fishhook" structure *accumulates* toward the "corner" of the homoclinic bifurcation set.

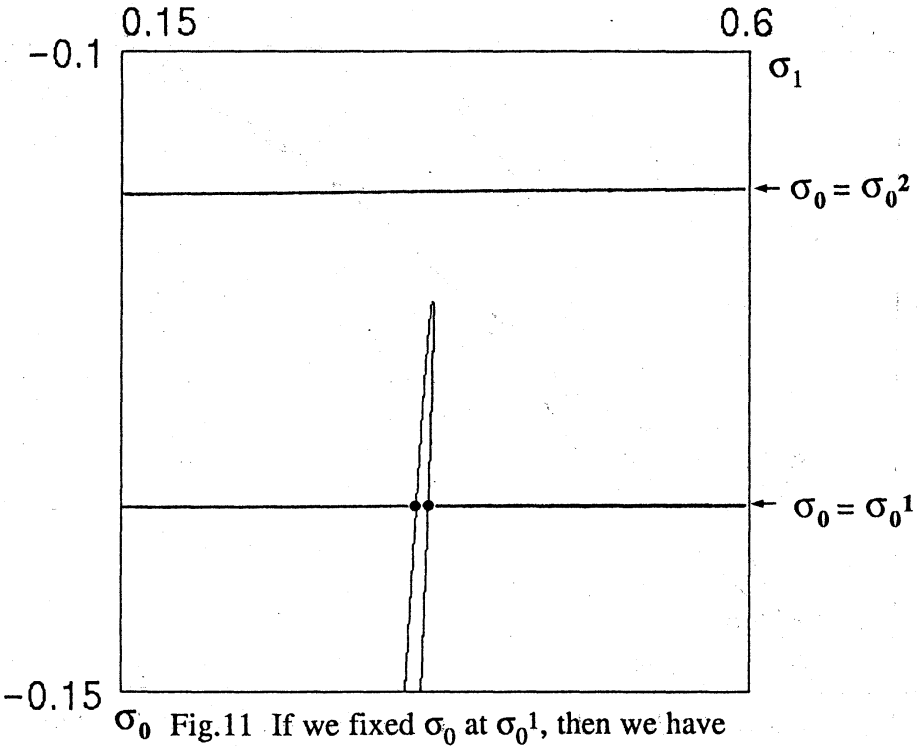

Fig.11 If we fixed σ_0 at σ_0^1, then we have two homoclinic orbit. But if we fixed σ_0 at σ_0^2, then we have no homoclinic orbit.

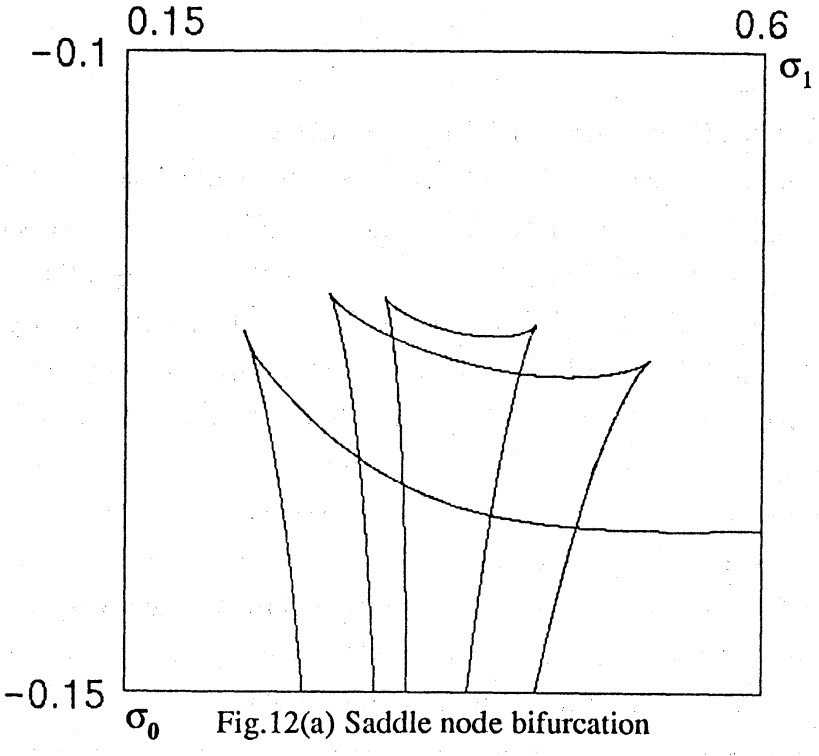

Fig.12(a) Saddle node bifurcation

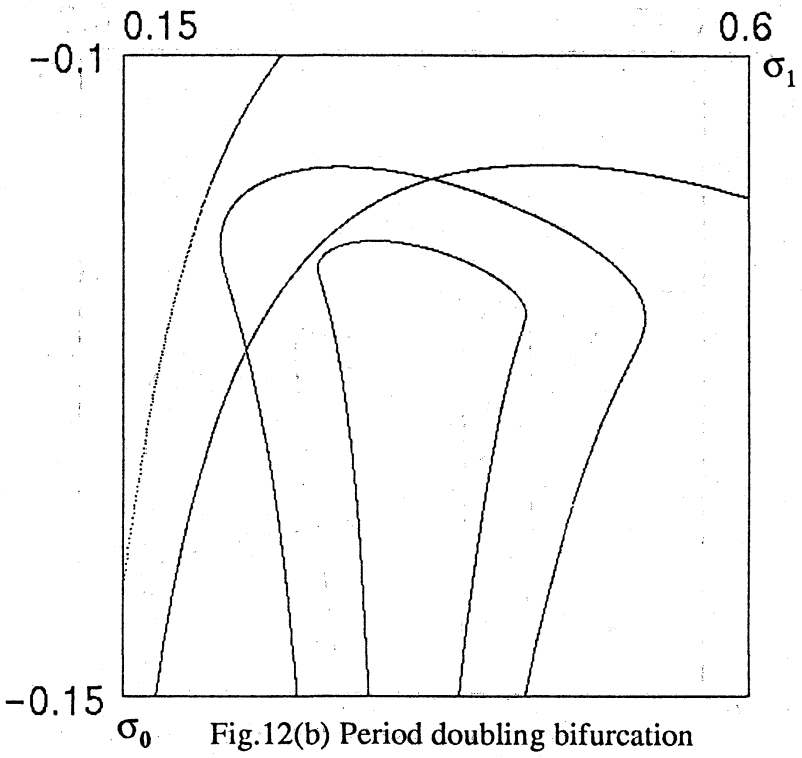

Fig.12(b) Period doubling bifurcation

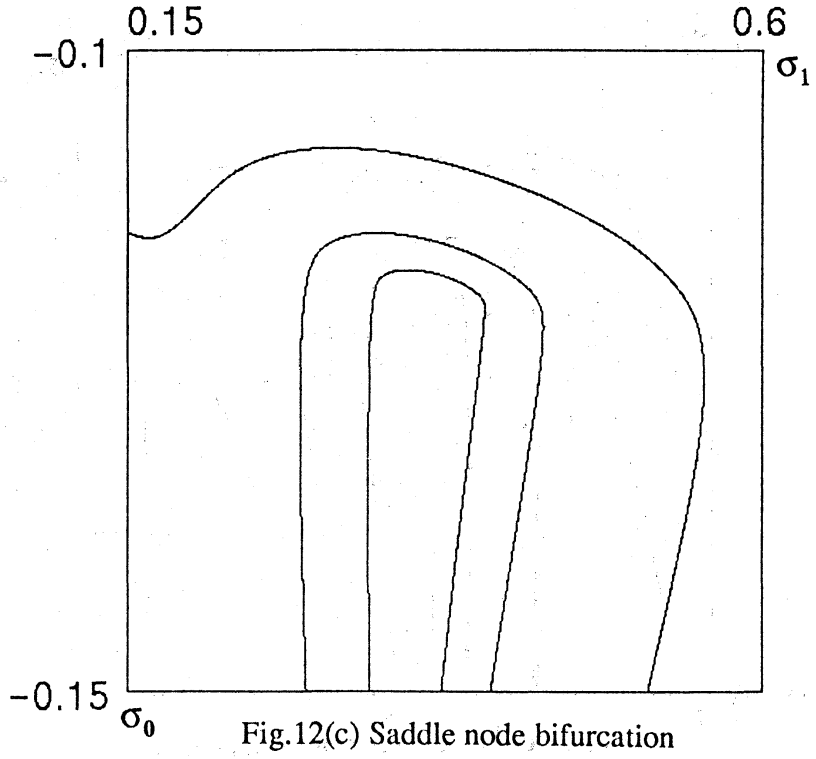

Fig.12(c) Saddle node bifurcation

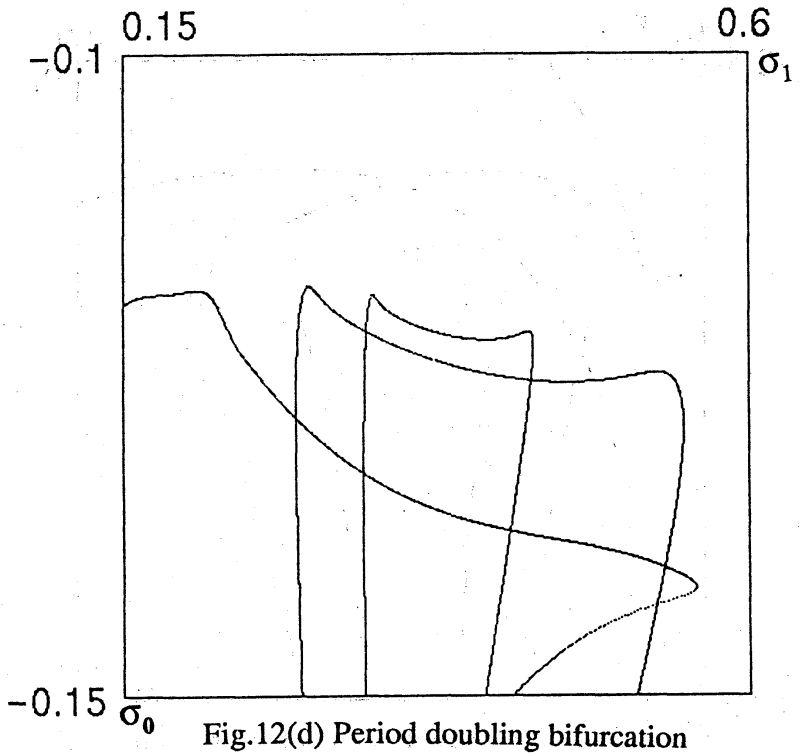

Fig.12(d) Period doubling bifurcation

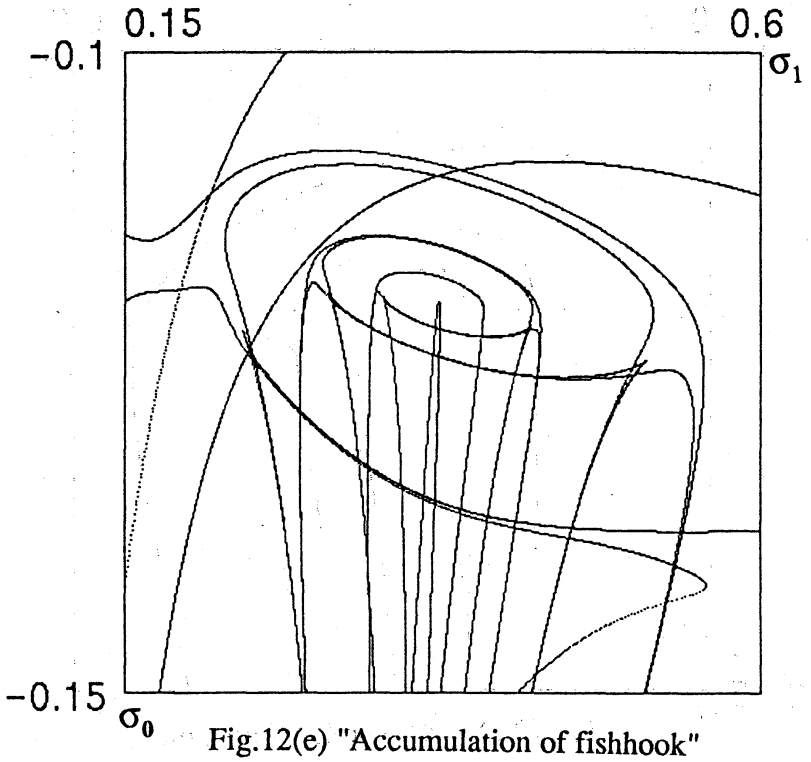

Fig.12(e) "Accumulation of fishhook"

4. MODEL BIFURCATION SET

Based on the previous discussions, Fig.13 shows a model bifurcation set describing all the details.

Finally, we remark that there have been previous works on the bifurcations near homoclinicities. [5]-[8]

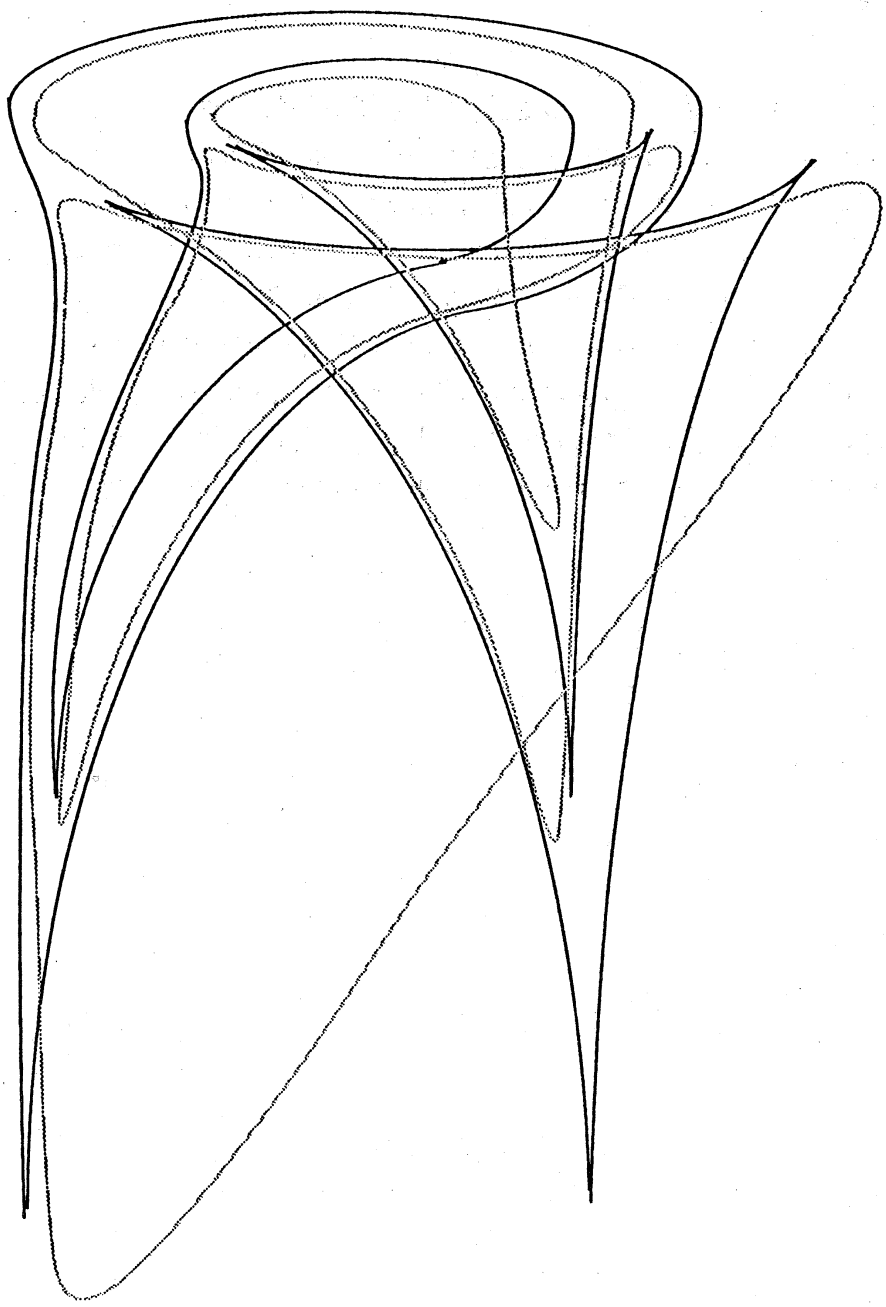

Fig.13 A schematic picture of global bifurcation

ACKNOWLEDGMENTS

We would like to thank Dr.H.Kokubu of Kyoto University, S.Takahashi, S.Higuchi of Waseda University for many stimulating discussions.

REFERENCES

[1] M.Komuro, Japan J. Appl. Math., Vol.5,no.2,pp257-304(1988)
[2] M.Komuro, Japan J. Appl. Math., Vol.5,no.3,pp503-549(1988)
[3] C.Tresser, Ann. Inst. Henri Poincaré, Vol.40,no.4,pp.441-461(1984)
[4] A.Arneod,P.Coullet,and C.Tresser,Commum. Math. Phys.,Vol.79,pp573-579(1981)
[5] P.Glendining and C.Sparrow, J. Stat. Phys.,Vol.35,nos.5/6(1984)
[6] P.Gaspard,R.Kapral and G.Nicolis, J. Stat. Phys.,Vol.35,nos.5/6(1984)
[7] L.O.Chua,M.Komuro and T.Matsumoto, IEEE Trans.Circuits Syst.,Vol.CAS-33,no.11(1986)
[8] R.Tokunaga,T.Matsumoto,M.Komuro,L.O.Chua.K.Miya,A.Hotta and R.Fujimoto, Proceedings of the IEEE International Symposium on Circuits and Systems,Vol.2(1989)